JBC Papers in Press. Published on February 16, 2017 as Manuscript M117.775205
The latest version is at http://www.jbc.org/cgi/doi/10.1074/jbc.M117.775205

Mycobacterium tuberculosis esxL inhibit MHC-II expression by promoting hypermethylation in class-II transactivator loci in macrophages

Srabasti Sengupta,[1] Saba Naz, [2] Ishani Das, [1] Abdul Ahad,[3] Avinash Padhi, [1] Sumanta Naik,[1] Geetanjali Ganguli, [1] Kaliprasad Patnaik, [1] Sunil Kumar Raghav,[3] Vinay Nandicoori [2] and Avinash Sonawane[1,] *

[1] School of Biotechnology, KIIT University, Bhubaneswar, Odisha, India

[2]National Institute of Immunology, New Delhi, India

[3] Institute of Life Science, Nalco Square, Bhubaneswar, Odisha, India

Running Title: Role of mycobacterial *esxL* in epigenetic modifications

***To whom correspondence should be addressed:** Dr. Avinash Sonawane, School of Biotechnology, Campus-11, KIIT University, Bhubaneswar, Orissa-751024, India, Phone: +91-674-2725349; Fax: +91-674-2725732 Email: asonawane@kiitbiotech.ac.in

Keywords: *Mycobacterium tuberculosis*, esxL, nitric oxide, histone trimethylation, CIITA, MHC-II, macrophages, p38-MAPK pathway

ABSTRACT

Mycobacterium tuberculosis (*Mtb*) is known to modulate the host immune responses to facilitate its persistence inside the host cells. One of the key mechanisms includes repression of class-II transactivator (CIITA) and MHC-II expression in infected macrophages. However, the precise mechanism of CIITA and MHC-II down-regulation is not well studied. *Mtb* 6-kDa early secretory antigenic target (ESAT-6) is a known potent virulence and antigenic determinant. *Mtb* genome encodes 23 such ESAT-6 family proteins. We herein report that *Mtb* and *M. bovis*-BCG infection down-regulated the expression of CIITA/MHC-II by inducing hypermethylation in histone H3 Lysine 9 (H3K9me2/3). Further, we show that *Mtb* ESAT-6 family protein EsxL, encoded by *Rv1198*, is responsible for the down-regulation of CIITA/MHC-II by inducing H3K9me2/3. We further report that *Mtb esxL* induced the expression of nitric oxide synthetase (iNOS), NO production and p38-MAPK pathway, which in turn was responsible for the increased H3K9me2/3 in CIITA via up-regulation of euchromatic histone-lysine N-methyltransferase 2 (G9a). In contrast, inhibition of iNOS, p38-MAPK and G9a abrogated H3K9me2/3 resulting in increased CIITA expression. Chromatin immune precipitation assay confirmed that hypermethylation at the promoter IV (pIV) region of CIITA is mainly responsible for the CIITA down regulation and subsequently antigen presentation. We found that co-culture of macrophages infected with *esxL* expressing *M. smegmatis* and mouse spleenocytes led to down-regulation of IL-2, a key cytokine involved in T-cell proliferation. In summary, we show that *Mtb esxL* inhibits antigen presentation by enhancing H3K9me2/3 on CIITA promoter thereby repressing its expression through NO and p38-MAPK activation.

INTRODUCTION

Pathogenic bacteria employ various host immune evasion strategies to facilitate its survival in the host cells. One of such mechanisms involves induction of epigenetic modifications in the host DNA, histone proteins and RNA by bacterial proteins (1, 2). Various bacterial virulent proteins have been shown to promote host chromatin and/or histone modifications via different signaling cascades. For example, *Shigella flexneri*, *Listeria monocytogenes* and *Helicobacter pylori* regulate p38 mitogen-activated protein kinase (MAPK) pathway by promoting histone 3(H3) phosphorylation and acetylation processes that subsequently modulate the secretion of various cytokines and chemokines in infected cells (3-5). *S. flexneri* infection inhibited MAPK dependent histone H3 serine 10 (H3S10) phosphorylation that impaired the recruitment of nuclear factor-kappa B (NF-κB) at the interleukin-8 (IL-8) promoter (4). On the other hand *L. monocytogenes* promoted H3K8 acetylation resulting in transcriptional activation of IL-8 via MAPK pathway (6, 7). Similarly *H. pylori* promoted NF-κB binding to the IL-6 promoter by inducing H3S10 phosphorylation via ERK and p38 (8, 5).

Tuberculosis (TB), caused by an intracellular pathogen *Mtb*, is a life threatening disease that infects 9 million people and kills more than 1.5 million people every year worldwide (9). According to the World Health Organization report, one-third of the global population is latently infected with *Mtb* but only 5 to 10 % of people with latent TB develop into an active TB disease (10). The underlying mechanisms responsible for this adaptation are poorly understood. Although, several reports are available on the correlation of other bacterial infections and epigenetics in the disease outcome, very little is known about the dynamics of epigenetic changes during mycobacterial infection. Macrophages, the primary host cells of *Mtb*, play a crucial role in recognition, phagocytosis and killing of mycobacteria. Non-pathogenic mycobacteria such as *M. smegmatis* (*Msm*) are readily killed by macrophages, whereas pathogenic mycobacteria (*Mtb*) are able to survive for extended period of time by manipulating the macrophage immune functions (11). These include prevention of phagolysosome fusion, inhibition of phagosome acidification due to depletion of vesicular proton-ATPase (V-ATPase), evasion from toxic effects of nitric oxide (NO) and reactive oxygen species (ROS), suppression of protective cytokine synthesis and T-helper (Th)-1 responses, and inhibition of apoptosis (12-15).

Recently, few reports have demonstrated that *Mtb* infection induces epigenetic modifications in host cells to aid its replication, propagation and protection from host immune responses (16,17,18). Mycobacterial cell wall protein, LpqH, was shown to block interferon-gamma (IFN-γ) induced

transcription of class-II transactivator (CIITA) by SWI/SNF binding and histone deacetylation at the CIITA promoter (19). IFN-γ induces the expression of major histocompatibility complex class II (MHC class II) by activating the transcription of CIITA (20). Another study has shown that *Mtb* downregulates HLA-DR transcription and MHC-II by inhibiting IFN-γ dependent histone acetylation and by recruiting mSin3A repressor at the HLA-DR promoter (21).

Inducible nitric oxide synthase (iNOS) catalyzes the formation of nitric oxide (NO), which helps in bacterial clearance, including *Mtb* (22, 23). It has been shown that NO knock-out mice were more susceptible to *Mtb* infection (24). In addition to its antibacterial properties, NO also mediate nitration, nitrosation and nitrosylation of key signalling molecules that determine the fate of macrophages and dendritic cells during bacterial infection (25-29). NO was shown to induce CIITA and MHC-II inhibition by signalling cross talks between NOTCH-PKCδ-MAPK-NFkβ-KLF4 pathway during *M. bovis* BCG infection (30).

Mtb early secretory antigenic target protein-6 (ESAT-6; esxA) is a known virulent as well as T-cell antigenic determinant (31). *Mtb* ESAT-6 was involved in the cytosolic escape of bacteria by inducing pore formation in the phagosomal membrane (32, 33). Previously, ESAT-6 protein was also reported to decrease histone H4 acetylation and H3K4 methylation at CIITA promoter (pI) (16). There are at least 23 such ESAT-6 family proteins present in the *Mtb* genome. However, the functions of many of them are still unknown. Herein, we showed that *Mtb esxL*, a previously uncharacterized member of ESAT-6 like family protein encoded by *Rv1198*, suppresses antimycobacterial defence mechanisms of macrophages by inhibiting the expression of CIITA and subsequently MHC-II molecules. Further mechanistic studies revealed that CIITA and MHC-II down-regulation by *esxL* was due to induction of H3K9 hypermethylation in the CIITA-IV promoter region (pIV), as determined by Western blotting and chromatin immuno-precipitation (ChIP) assays. We further showed that recombinant *M. smegmatis* expressing *esxL* (*Msm esxL*) induced the synthesis of p38 MAPK, iNOS and NO that promoted H3K9me2/3 at the CIITA promoter via up-regulation of G9a (also known as euchromatic histone-lysine N-methyltransferase2 , EHMT2), whereas *Mtb* Δ*esxL* mutant down-regulated H3K9me2/3. EsxL mediated H3K9me2/3 also resulted in inhibition of antigen presentation and secretion of interleukin-2 (IL-2), a key cytokine involved in T-cell activation. In summary, we identified another mechanism by which *Mtb* aids its persistence by repressing CIITA/MHC-II via G9a, p38 and NO dependent H3K9me2/3 in promoter IV of CIITA.

RESULTS

M. smegmatis esxL showed prolonged intracellular survival in RAW 264.7 and THP-1 cells

Mtb ESAT-6 is known as a potent virulence as well as antigenic determinant (31, 34). Recently, we have shown that *Mtb* Rv2346c, a member of ESAT-6 like family proteins, endow bacterial persistence by dampening the antibacterial effector functions by inducing genomic instability and autophagy in macrophages (35). Using *Msm* as a surrogate model, we (35, 36, 37) and several other groups (38, 39) have proved the functions of several *Mtb* proteins in pathogenesis. Similarly, in this study we ectopically expressed one of the *Mtb* ESAT-6 family proteins EsxL, encoded by *Rv1198*, in *Msm* (*Msm esxL*) and also constructed *Mtb esxL* deletion mutant (*Mtb* Δ*esxL*) and studied its role in pathogenesis. Figure 1A shows genetic organization of *esxL* in the *Mtb* genome. It is located downstream of another ESAT-6 like protein esxK, encoded by *Rv1197*. *esxL* has previously been identified from the membrane fraction (40) and culture filtrates (41) of *Mtb* with unknown function. It was reported that immunization of BALB/c mice with Rv1198 induced a pro-inflammatory response with elevated levels of tumor necrosis factor-alpha (TNF-α) and IL-6, along with low induction of IFN-γ, IL-2 and IL-10 (42). EsxL has been assigned to a member of Rv1793, Rv1037c and Rv2346c, all belonging to the ESAT-6 family proteins (43). Despite of these important characteristics shown by *esxL*, its role in pathogenesis is still unknown. Comparative genome analyses revealed that *M. bovis*-BCG genome contain Mb1230, an orthologue of *Mtb* esxL; while *Msm* genome does not contain any esxL orthologue (Tuberculist database).

As esxL was found to be a member of ESAT-6 family protein that is known as a key

virulence factor, we compared the intracellular bacillary persistence of *Msm* harboring pSMT3 vector (*Msm* pSMT3) and *Msm* expressing *esxL* (*Msm esxL)* strains in mouse macrophage RAW 264.7 and PMA differentiated THP-1 cells. The infected cells were lysed at different time points post-infection and the bacterial survival was determined by colony forming unit (CFU) enumeration. The bacterial input and time zero (T_0) counts were determined to calculate the intracellular bacterial survival. The recombinant *Msm esxL* showed significantly high bacterial burden in RAW 264.7 ($P \leq 0.001$; Figure 1B) and THP-1 cells ($P \leq 0.001$; Figure 1C) when compared with *Msm* pSMT3 strain after 24 h of infection. We did not observe any differences in the growth patterns of *Msm* wild-type *(Msm* WT), *Msm* pSMT3 and *Msm esxL* strains (Figure 1D) suggesting that the observed increased bacterial survival was not due to differences in the growth kinetics of bacteria. The intracellular and extracellular expressions of *esxL* were determined by qRT-PCR at 4, 12 and 24 h time points. As shown, *esxL* was expressed under both *in-vitro* (Figure 1E) and *ex-vivo* (Figure 1F) conditions. In conclusion, above data showed that *Mtb esxL* has a role in increased bacterial persistence inside the macrophages.

EsxL induced NO production and iNOS expression in macrophages

iNOS, which catalyzes the formation of NO, perform immunomodulatory activities that determine the outcome of *Mtb* infection (45). In addition to its antibacterial properties, NO is also known as a key regulator in initiation and maintenance of anti-TB protective immunity (46) and to modulate the cellular signaling pathways that can either support or inhibit the bacterial growth depending up on the cytokine milieu (47). Previously, ESAT-6 was shown to induce NO production in macrophages (48). We found significantly higher NO production in *Msm esxL* infected RAW 264.7 cells as compared to *Msm* pSMT3 infected cells at the indicated time points ($P \leq 0.05$ and $P \leq 0.01$; Figure 2A). Similarly, we observed approximately 18-fold increase in *iNOS* at transcriptional ($P \leq 0.001$; Figure 2B) and translational levels (Figure 2C) in *Msm esxL* infected macrophages. Immunofluorescence studies using iNOS specific antibody also showed significantly increased expression in *Msm esxL* infected macrophages as compared to uninfected and *Msm* pSMT3 infected cells (Figure 2D). On the contrary, decreased iNOS expression was observed in *Mtb* Δ*esxL* infected THP-1 cells when compared with *Mtb* infected cells (Figure 2E). The generation of *Mtb* Δ*esxL* is shown in Fig 1G and H. We did not observe any significant differences in the production of reactive oxygen species (ROS) in infected macrophages (data not shown) indicating that *Mtb esxL* specifically induces NO production in macrophages.

EsxL down-regulated MHC-II and CIITA in macrophages

Pathogenic mycobacteria are known to down-regulate the surface expression of MHC-II molecules in macrophages (49). The MHC-II dependent antigen presentation is tightly regulated by a key transcription factor class II transactivator (CIITA). Mice deficient for CIITA showed a marked reduction in MHC-II expression (50). It has been shown that *M. bovis*-BCG infection inhibited MHC-II expression by inducing the NO production in macrophages (30). In view of these reports, we checked the expression of MHC-II and CIITA in *Mtb, Mtb* Δ*esxL*, *Msm* pSMT3 and *Msm esxL* infected macrophages. As shown, *Msm esxL* infection abrogated CIITA expression at both transcriptional ($P \leq 0.01$; Figure 3A) and translational levels (Figure 3B). *Mtb* infected THP-1 cells also showed time-dependent decrease in CIITA expression (Figure 3C), whereas increased CIITA expression was observed in *Mtb* Δ*esxL* infected cells (Figure 3D). We further confirmed the effect of CIITA on MHC-II expression. A significant decrease in MHC-II expression was observed at both transcriptional ($P \leq 0.01$; Figure 3E) and translational (Figure 3F) levels in *Msm esxL* infected RAW264.7 macrophages when compared with *Msm* pSMT3 infected cells. Flow cytometry analysis also showed a significant decrease in MHC-II expression in *Msm esxL* infected THP-1 (Figure 3G) and RAW264.7 macrophages (Figure 3H). In agreement with previous reports, we also observed time dependent decrease in MHC-II expression in *Mtb* infected THP-1 cells (Figure 3I) when compared with *Mtb* Δ*esxL* infected cells (Figure 3J). Altogether, these data suggest that *Msm esxL, M. bovis*-BCG and *Mtb*

mediated MHC-II inhibition is due to down-regulation of CIITA levels.

M. smegmatis esxL infection down-regulated IL-2 and IL-10 and up-regulated IL-6 and TNF-α production in macrophages

It is known that inhibition of antigen presentation prevents T-cell activation (51). As mentioned above, IL-2 is a key cytokine involved in T-cell activation (52, 53). Therefore, we checked IL-2 levels using Bioplex cytokine analysis kit. For this macrophages were first infected with *Msm* pSMT3 and *Msm esxL* strains followed by co-culture with BALB/c mice spleenocytes. We found significant down-regulation of IL-2 ($P \leq 0.05$, Figure 4A) and IL-10 ($P \leq 0.05$, Figure 4B) cytokines in supernants obtained from *Msm esxL* infected cells as compared to *Msm* pSMT3 infection after 24 h. However, treatment with G9a inhibitor UNC0638 increased the production of both cytokines suggesting that *Msm esxL* infection suppressed T-cell activation. In contrast, TNF-α ($P \leq 0.01$, Figure 4C) and IL-6 ($P \leq 0.01$, Figure 4D) were up-regulated in *Msm esxL* infected cells.

M. smegmatis esxL induce histone modification (H3K9 hypermethylation) in macrophages

Few studies have shown that pathogenic mycobacteria and its antigens induce epigenetic changes to evade host immune responses (16, 19, 53). We hypothesized that esxL might render repressive epigenetic modifications at the CIITA promoter that subsequently inhibit MHC-II dependent antigen presentation. H3K9me2/3 is involved in transcriptional repression (54). Therefore, we analyzed the status of H3K9me2/3 in infected macrophages. Indeed, immuno-blotting (Figure 5A) and immuno-fluorescence (Figure 5B) analysis showed significantly elevated levels of H3K9me2/3 in *Msm esxL* infected macrophages as compared to control cells. A significant increase in H3K9me2/3 puncta was observed in *Msm esxL* infected cells. We did not observe any significant differences in H3K4me3 and total H3 in *Msm* pSMT3 and *Msm esxL* infected macrophages (Figure 5C) indicating that *esxL* induce H3K9me2/3 in macrophages.

M. bovis BCG and M. tuberculosis infection also induce H3K9me2/3 in macrophages

To further confirm the role of *esxL* in inducing repressive histone modification, we analyzed the expression of H3K9me2/3 in *M. bovis*-BCG, *Mtb* and *Mtb* Δ*esxL* infected macrophages. Concordantly, Western blot analysis showed increased levels of H3K9me2/3 in *M. bovis* BCG (Figure 5D) and *Mtb* (Figure 5E) infected macrophages suggesting that *Mtb* and BCG may down-regulate CIITA expression by inducing H3K9me2/3 in macrophages. In contrast, decreased H3K9me2/3 expression was observed in *Mtb* Δ*esxL* infected THP-1 cells when compared with *Mtb* infected cells (Figure 5F).

M. smegmatis esxL and M. bovis-BCG induce H3K9me2/3 modification by up-regulating EHMT2 methyltransferase activity

To further investigate the mechanism of H3K9me2/3 induction, we studied the activity of methyltransferases in infected macrophages. Several H3K9-specific lysine methyltransferases such as Eset, KMT1E, G9a are involved in H3K9methylation (55). Among them, G9a also known as euchromatic histone-lysine N-methyltransferase 2 (EHMT2), is a dominant histone methyl transferase responsible for methylation of H3K9 (56). Transcriptional analysis showed significant increase in G9a level in *Msm esxL* ($P \leq 0.01$; Figure 5G) and *Mtb* ($P<0.001$; Figure 5H) infected THP-1 cells, whereas *Mtb* Δ*esxL* infection down-regulated G9a expression ($P<0.001$; Figure 5H). Otherwise, treatment with G9a inhibitor (UNC0638) subdued the expression of H3K9me2/3 in *Msm esxL* infected macrophages when compared with untreated cells (Figure 5I). Similar results were obtained with *M. bovis*-BCG infection. In which, BCG infection increased the level of H3K9me2/3, while treatment with G9a inhibitor reduced H3K9me2/3 level (Figure 5D). Collectively, these results indicate that *Msm esxL*, *Mtb* and *M. bovis*-BCG induce H3K9me2/3 via G9a methyltranferase.

To assess whether CIITA down-regulation during *Msm esxL* infection is dependent on G9a mediated H3K9me2/3, we checked the expression of CIITA in untreated and G9a inhibitor treated macrophages. Immunoblot analysis showed that pretreatment with G9a inhibitor severely reduced the capacity of *Msm esxL* to inhibit CIITA expression in macrophages (Figure 5I) indicating that observed CIITA down-regulation was due to

G9a dependent induction of H3K9me3 in infected macrophages.

ChIP analysis showed that H3K9 hypermethylation occurs at promoter IV region of CIITA

ChIP assay was performed to check H3K9me2/3 in CIITA promoter. Sequence analysis revealed the presence of three promoter regions (CIITApI, CIITApIII and CIITApIV) in CIITA. As shown, *Msm esxL* down-regulated CIITA expression by inducing H3K9me2/3 at promoter IV region of CIITA ($P \leq 0.001$; Figure 5J), while no such induction was observed in CIITApI and CIITApIII promoters (data not shown). Moreover, we did not observe any H3K9me2/3 enrichment in *Msm* pSMT3 infected cells. Importantly, inhibition of G9a significantly decreased H3K9 hypermethylation at CIITA promoter IV in *Msm esxL* infected macrophages ($P \leq 0.01$; Figure 5K).These results clearly indicate that *Msm esxL* down-regulate G9a dependent CIITA expression by promoting H3K9me2/3 in promoter IV region of CIITA.

M. smegmatis esxL trigger H3K9me2/3 mediated CIITA inhibition by inducing MAPK signaling pathway

NO acts as a key intermediate in regulation of cell-fate decisions by modulating several signaling pathways in the host cells (57, 58). Hence, we postulated that signaling cascades that regulate NO production could act as a focal point in *Msm esxL* infection-triggered histone modification that subsequently leads to inhibition of MHC-II or CIITA. Mitogen-activated protein kinase (MAPK) pathways are known to regulate eukaryotic gene expression by modulating the chromatin structure of regulatory elements (59). Increased MAPK leads to recruitment of HDACs leading to gene repression (60). Mycobacteria, in addition to selective antigens, are known to induce MAPK signaling in macrophages (61). In this context, we addressed the role for MAPK signaling pathway in the regulation of H3K9me2/3 and CIITA expression. We found that *Msm esxL* infection triggered the activation of p-P38 (Figure 6A) and p-ERK (Figure 6B) when compared with control conditions. Similarly *Mtb* infection also induced p-P38 expression when compared with *Mtb* Δ*esxL* infected THP-1 cells (Figure 6C). Importantly, pretreatment with p38 inhibitor (SB203580) abrogated the *Msm esxL* induced inhibition of CIITA (upper panel, Figure 6D). Similarly, treatment with SB203580 down-regulated the expression of H3K9me2/3 in *Msm esxL* infected macrophages (middle panel, Figure 6D). On the other hand, inhibition of p-ERK by the pharmacological inhibitor U0126 did not show any effect on the expression of both CIITA and H3K9me2/3 during *Msm esxL* infection when compared with untreated macrophages (Figure 6E). These results clearly suggest that *Msm esxL* triggered P38 MAPK signaling pathway hold the capacity to modulate H3K9me2/3 expression to regulate CIITA/MHC-II expression.

Msm esxL induced NO production regulates induction of H3K9me2/3 and inhibition of CIITA expression

Next, we assessed the role of iNOS/NO during *Msm esxL*-infection in modulating the expression of H3K9me3 and CIITA. For this, macrophages were infected with *Msm* pSMT3 and *Msm esxL* strains and then treated with an iNOS inhibitor 1400W. Treatment with 1400W inhibitor severely down-regulated the expression of H3K9me2/3 in *Msm esxL* infected macrophages (Figure 6F). On the other hand, inhibition of iNOS led to increased expression of CIITA when compared with untreated conditions (Figure 6F). These results confirm the crucial role of NO in repression of CIITA by increasing hypermethylation of H3K9.

DISCUSSION

Mtb adopt various strategies to evade host defense mechanisms to facilitate its survival in the host cells. One such mechanism involves epigenetic modifications in the host proteins to dampen antibacterial effector functions of host cells. In this context, various *Mtb* proteins including ESAT-6, CFP-10, lipoproteins and PE/PPE proteins are known to be involved in the establishment of infection process (62-70). Herein, we report that *Mtb esxL* repress CIITA/MHC-II expression by inducing H3K9me2/3 in CIITA promoter.

Previously we and several other studies have used *Msm* as a surrogate model to elucidate the function of *Mtb* proteins in pathogenesis. For example, expression of *Mtb* Mce4A protein in a non-pathogenic *Escherichia coli* increased invasion

in HeLa cells (71), while expression of *Mtb* PE proteins in *Msm* increased its virulence properties (72). Based on these evidences, we expressed *Mtb esxL* in *Msm* strain and also deleted *esxL* from *Mtb* genome (*Mtb* Δ*esxL*) and proved its function using macrophage infection model.

Msm genome does not contain esxL orthologue, therefore, the observed phenotypes can be attributed to the ectopic expression of *esxL* in *Msm*. Using human and mice macrophage infection models we showed that recombinant *Msm esxL* strain survive more as compared to control strains indicating that *esxL* is involved in bacillary persistence in macrophages. It is well established that pathogenic *Mtb* facilitate its survival by modulating ROS and NO production (73-76). We observed that *Msm esxL* strain increased NO and iNOS production in infected macrophages, while inhibition of iNOS decreased the intracellular survival of *Msm esxL*. Contrary, *Mtb* Δ*esxL* reduced iNOS expression. The role of NO as an antimicrobial agent has been extensively studied in the context of host defense mechanisms. Nevertheless, previous study has provided evidence that reactive nitrogen intermediate (RNI) help in proliferation of *Mtb* suggesting bacteriostatic effect of RNI on *Mtb* (77). In addition to antimicrobial properties, NO/iNOS are also known to modulate several signaling cascades that regulate cell fate decisions of host cells (56, 58). Previous studies have shown that *Mtb* down-regulates CIITA thus altering antigen presentation (78). However, specific *Mtb* protein responsible for observed down-regulation was not known. Our study has provided several evidences that esxL could be responsible for CIITA down-regulation. It has been shown that epigenetic modifications are involved in regulating CIITA expression (49, 79, 80). Studies also showed that *Mtb* proteins like LpqH and ESAT-6 cause CIITA inhibition by decreasing histone H3K4 methylation level and acetylation levels (16,19). Our study has unambiguously shown that *Mtb esxL* induced H3K9me2/3 in host cells. H3K9me1/2/3 is known for transcriptional repression of the gene which undergoes modification at its promoter region (54, 42). We have further provided evidences that *esxL* induced H3K9me2/3 are mediated via G9a, which is a known histone methyl transferase responsible for H3K9 methylation. Inhibition of G9a down-regulated H3K9me2/3 and simultaneously resulted in up-regulation of CIITA indicating that G9a methyl transferase is responsible for H3K9 hypermethylation in CIITA promoter. Indeed, ChIP assay showed that *Mtb esxL* promoted H3K9me2/3 at the promoter IV region of CIITA gene, which led to the transcriptional repression of CIITA that subsequently perturbed antigen presentation and T-cell activation. Level of H3K9me2/3 was also found to be increased in *M. bovis*-BCG and *Mtb* infected macrophages, whereas levels of H3K9me2/3, CIITA, MHC-II, iNOS and P38 was down-regulated in *Mtb* Δ*esxL* infected macrophages. *M. bovis*-BCG contains esxL orthologue, Mb1230. Therefore, *M. bovis* BCG induced H3K9me2/3 could be attributed to this protein.

MAPK signaling pathway plays a crucial role in mycobacterial infection. *Mtb* 38-kDa protein was shown to induce TNF-α and IL-6 through MAPK pathway to facilitate mycobacterial infection (42). As shown before, MAPK components ERK and P38 are known to alter gene transcription by altering chromatin structure (59). The recruitment of HDACs at promoter site of the gene is known to be facilitated by MAPK (60). In our study, we found that *Msm esxL* infection upregulated ERK and p38 levels in macrophages. However, inhibition of p38 downregulated the expression of H3K9me2/3 and CIITA indicating that esxL induced H3K9me2/3 is mediated via p38 signaling pathway. Previous studies have shown the involvement of p38 in repressive epigenetic modification. *Mtb* LpqH activates p38, which in turn facilitates the recruitment of HDAC to the promoter of CIITA, thus repressing gene transcription (19). We further showed that esxL induced H3K9me2/3 is dependent on NO production. There are reports suggesting the involvement of NO/iNOS in downregulation of CIITA. A study has shown that BCG infection increased NO production that upregulated the expression of KLF4 transcription factor. KLF4 acts as a regulatory switch and inhibits CIITA expression (30).

In summary, we have studied a mechanism in detail that leads to repression of CIITA/MHC-II during *Mtb* infection. Figure 7 shows schematic representation of a mechanism that leads to repression in antigen presentation and T-cell activation by inducing H3K9me2/3 in promoter IV

region of CIITA via NO, p38-MAPK and G9a during infection.

EXPERIMENTAL PROCEDURES

Chemicals, reagents and cell culture conditions

Mycobacterium smegmatis mc^2155 was grown in Middlebrook's 7H9 broth medium (Difco) containing 0.05% Tween 80, 0.5% glucose and 0.5% albumin at 37 ^{0}C on a shaker at 120 r.p.m. *M. tuberculosis* H37Rv and *M. bovis* BCG were grown in Middlebrook's 7H9 broth medium (Difco) containing 0.05% Tween 80, 0.5% glucose, 0.5% albumin and Oleic Albumin Dextrose Catalase (OADC) at 37 ^{0}C on a shaker at 120 r.p.m. *Escherichia coli* XL-10 Gold (Stratagene) was grown in Luria-Bertani (LB) broth supplemented with 20 µg/ml tetracycline. pSMT3 vector was a kind gift from Dr. Rakesh Sharma (IGIB, Delhi). Murine RAW264.7 macrophage cell line was cultured in DMEM Dulbecco's modified Eagle's medium (DMEM; HiMedia, Mumbai, India) supplemented with 10% fetal bovine serum, 1% penicillin-streptomycin solution, and 1% L-glutamine. THP-1 cells (70) were grown in RPMI 1640 (Gibco) supplemented with 10% FBS, 10 mM HEPES, 1 mM sodium pyruvate and penicillin-streptomycin solution. The cells were seeded onto 24-well culture dishes at a density of $2x10^5$ cells/ml and treated overnight with 20 nM phorbol myristate acetate (PMA) (Sigma) for 24 h. Cells were then washed three times with PBS and incubated for one more day before performing the experiment. Anti-iNOS, anti- H3K9me3, anti- phospho –p38, anti-phospho- ERK1/2, anti- histone H3, anti- β-actin, anti-GAPDH and secondary goat anti- rabbit and goat anti-mouse antibodies were purchased from Cell Signaling Technologies (USA). Anti- CIITA antibody was purchased from Abcam (UK). Anti-MHC-II and anti-mouse IgG were procured from Santa-cruz (USA). FITC-labelled anti-human MHCII antibody was purchased from Invitrogen (USA). Goat anti-mouse IgG, Alexa Fluor 633, goat anti-rabbit IgG, Alexa Fluor 488 secondary antibodies were purchased from Thermofisher Scientific (USA). Mounting solution with DAPI was purchased from DAKO (USA). All the pharmacological inhibitors were purchased from Sigma (USA) and Calbiochem (USA) and reconstituted in DMSO (Himedia, India) or sterile H_2O at the following concentrations: 1400W (100 µM), U0126 (10 µM), SB203580 (10 µM), and UNC0638 hydrate (5µM).

Cloning and expression of esxL

Mycobacterium tuberculosis esxL was PCR amplified using gene specific primers (Table 1) and *Mtb* genomic DNA as template. The PCR amplified products were gel purified, sequentially digested with *Pst*I and *Hind*III and cloned into pSMT3 shuttle vector. The recombinant constructs were transformed into competent *E. coli* XL-10 gold. The positive clones were selected on LB agar plates supplemented with 20µg/ml tetracycline and 50 µg/ml hygromycin. The positive clones were confirmed by colony PCR and sequencing using gene specific primers. Finally the recombinant constructs were transformed into electrocompetent *M. smegmatis*. The positive colonies were selected on 7H9 medium containing 50 µg/ml hygromycin B. The positive transformants were confirmed by colony PCR and sequencing using gene specific primers.

Generation of M. tuberculosis esxL mutant

Temperature sensitive phage based transduction methodology was used for the generation of *Mtb esxL* deletion mutant (Figure 1G and H). Upstream (814 bp) and downstream (812 bp) flank regions were PCR amplified and the amplicons were digested with *PflMI* restriction enzyme. Flanks were ligated with the compatible *sacB+hyg*^{r} and *oriE+λcos* fragments from pYUB1471to generate Allelic Exchange Substrate (AES). AES was packaged into phAE159 phasmid (A kind gift from Dr. William Jacob's Lab) and high titer phages were generated and transduced into *M. tuberculosis* H37Rv harboring pNit-ET plasmid as describe earlier (44).

Intracellular bacterial survival assay

M. smegmatis wild-type (Msm WT), *Msm* harboring plasmid pSMT3 *(Msm* pSMT3) and recombinant *Msm* expressing *Mtb esxL (Msm esxL*) strains were grown to mid-exponential phase. Then bacterial cultures were pelleted, washed in 1X PBS and re-suspended in DMEM medium to a final OD_{600} 0.1. Bacterial clumps were broken by ultrasonication for 5 min followed by a low speed centrifugation for 2 min. RAW264.7 macrophages ($2x10^5$ cells/well) were seeded on 24-well tissue culture plates with media containing no antibiotic solution and grown

for 18-20 h. Cells were infected with *Msm* WT, pSMT3 and *Msm esxL* strains at an MOI 10 and intracellular survival was determined by lysing the infected macrophages at different time points and bacterial survival was determined by plating the serially diluted samples onto 7H9 plates after lysing the cells with 0.5% Triton-X 100. The equal input and time zero (T_0) counts of infecting bacilli were determined to calculate the percentage survival. % survival= CFU at required time / CFU of bacteria added X 100. For THP-1 infection assay, cells were first treated with 20 nM phorbol myristate acetate (PMA) (Sigma) in RPMI medium and the infection assay was performed as described above.

Intracellular expression of esxL

RAW 264.7 macrophages were infected with *Msm esxL*, RNA was isolated at 4, 12 and 24 h time points followed by cDNA synthesis. qRT-PCR was performed using the cDNA as templates using gene specific primers (Table 1). *SigA* was used as an internal control.

Extracellular expression of esxL

Msm esxL strain was grown *in-vitro* for 24 h in 7H9 broth constituted with 0.05% Tween80 under shaking condition. Cell pellets were harvested followed by RNA isolation and cDNA synthesis. qRT-PCR was performed using gene specific primers and cDNA as template. *SigA* was used as an internal control.

Infection with M. tuberculosis H37Rv and Mtb ΔesxL

THP1 cells were maintained in RPMI 1640 supplemented with 10% heat inactivated FBS and differentiated using PMA. The infection experiment with *Mtb H37Rv* or *Mtb ΔesxL* strains was performed as described earlier (82). For the lysate preparation, 8×10^6 cells were seeded in 10 cm cell culture dishes and the infection was performed at 1:5 multiplicity of infection (MOI). At different time points cells were washed with PBS and lysed by using 600 µl of RIPA buffer, vortexed for 30 second and kept in ice. The procedure was repeated thrice and the cell lysates were clarified at 13000 rpm at 4^0C.

Free Nitric Oxide (NO) estimation

RAW264.7 ($2x10^5$cells/well) was seeded on 24-well plates. Next day, the cells were infected with *Msm* WT, pSMT3 and *Msm esxL* strains for 24 h. The accumulation of nitrite was measured by mixing 100 µl of culture supernatants with an equal volume of Griess reagent (1% sulfanilamide– 0.1% naphthylethylenediamine dihydrochloride in 5% concentrated H_3PO_4) in 96-well plates. The plates were incubated for 10 min at room temperature and absorbance was measured at 550 nm in a microtiter plate reader (EPOCH, BioTek, USA). The nitrite concentrations (in micromoles per sample) were determined by a least-square linear regression analysis using sodium nitrite as a standard (5 to 100 µM range). The values were averaged from three independent experiments.

RNA isolation and Quantitative Real-time RT-PCR

Total RNA was isolated from infected or uninfected macrophages using TRIzol reagent (Invitrogen) as per the manufacturer's protocol. The cDNA synthesis kit (Thermofisher Scientific) was used for reverse transcription according to the manufacturer's protocol. Quantitative real time RT-PCR amplification using the SYBR Green PCR mixture (KAPA Biosystems) was performed for quantification of target gene expression in Real Plex master cycler (Eppendorf, Germany) with initial denaturation at 95 ^{o}C for 10 min, final denaturation at 95 ^{o}C for 30 s, annealing at 52 ^{o}C for 30 s and extension at 72 ^{0}C for 30 s to generate 200 bp amplicons. All reactions were repeated at least twice independently to ensure reproducibility of the result. The mRNA levels were normalized to the transcript levels of GAPDH and the relative fold changes were calculated.

Western blot analysis

RAW264.7 cells were infected with *Msm* WT, pSMT3 and *Msm esxL*. After 24 h of infection, protein samples were prepared by cell lysis using RIPA buffer (HiMedia) containing 5mM EDTA, 5mM EGTA, 1 mM PMSF, protease inhibitor cocktail, 50mM NaF, 1mM DTT, 1mM Sodium orthovanadate. Proteins were electrophoresed in 12% SDS-PAGE and transferred to polyvinylidene difluoride membrane (PVDF) (GE Healthcare Life sciences) overnight at 28 Volts. Then the blots were blocked with 5% BSA or skimmed milk in TBST (20 mM Tris-HCl, pH 7.4, 137 mM NaCl, and 0.1% Tween 20) for 60 min. Then blots were incubated with primary rabbit IgG antibodies (1:1000)

overnight at 4 ºC and then with HRP-conjugated anti-rabbit or anti-mouse IgG secondary antibodies in 5% BSA or skimmed milk (1:1000) for 2 h. The membrane was washed using 1X TBST and X-ray film was developed using standard chemiluminescent solvent. β-actin and GAPDH were used as loading controls.

Immunofluorescence

For immunofluorescence studies, RAW 264.7 macrophages ($5X10^4$) were seeded on coverslips. After infecting the cells with *Msm* pSMT3 and *Msm esxL*, cells were fixed with acetone: methanol (1:1) for 20 min at -20^0C and then blocked with 5% BSA for 1h at room temperature and stained with primary anti-iNOS and anti-H3K9me3 antibodies overnight in dark. Then the coverslips were stained with secondary antibodies for 2 h at room temperature. Finally the cells were mounted in mounting solution with DAPI and the images were analyzed using BX61 Olympus fluorescence Microscope and Cytovision Software7.2.

Flow cytometry analysis

For flow cytometry analysis, THP-1 ($2X10^5$) and RAW 264.7 ($2X10^5$) cells were seeded onto 24-well cell culture plates. Cells were infected with *Msm* pSMT3 and *Msm esxL* for 24 h. The cells were then harvested and blocked with 0.1% BSA for 15 min on ice. The cells were then centrifuged at 2500 r.p.m. for 5 min followed by staining with primary FITC-labelled anti-human MHC-II and anti-mouse MHC-II antibodies for 30 min on ice and then with secondary antibodies. Untreated cells were taken as negative controls. Flow cytometry was performed by analyzing 10,000 gated cells using a FACS Canto II flow cytometer and FACS Diva software.

Chromatin immunoprecipitation (ChIP) assay

For ChIP assay, RAW 264.7 ($1X10^7$) cells were seeded onto 100 mm tissue culture disks. Cells were infected with *Msm* pSMT3 and *Msm esxL*. For ChIP assay with G9a inhibition, RAW 264.7 were infected with *Msm esxL* and then treated with G9a inhibitor, UNC0638. After 24 h of infection cells were washed twice with 1X PBS and then crosslinked with 11% formaldehyde solution for 15 min followed by 2.5M glycine treatment for quenching formaldehyde solution. The cells were then washed with ice cold 1X PBS twice. The cells were then harvested by scrapping using ice cold 1X PBS and centrifuged at 2500 r.p.m. for 5 min at 4 ºC followed by washing with 1X PBS. The pellets were then resuspended with ice cold 1ml Farnham buffer and then centrifuged at 2000 r.p.m. for 5 min at 4 ºC. The pellet was resuspended with 300 µl of RIPA buffer and then kept on ice for 10 min followed by sonication in Bioruptor at high setting for a total time of 40 min, 30 seconds ON, 30 seconds OFF at 4ºC. The chromatin length was then verified and proceeded for further steps. The sonicated mixture was centrifuged at 14000 r.p.m. for 15 min at 4ºC. The supernatant was collected, quantified and adjusted the volume with RIPA buffer so that each reaction has 150 µg/ml of chromatin. The suspension was then incubated with previously prepared Protein-A sepharose beads for 1h at 4ºC in rotator. After centrifugation at 1500 r.p.m. for 2 min at 4ºC, the supernatant was taken and incubated overnight with 6µg of antibodies against H3K9me2/3 and mouse IgG per IP at 4ºC for in rotator. Next day, the suspensions were again incubated with Protein-A sepharose beads at 4ºC for 2 h in rotator and then centrifuged at 2000 r.p.m. for 1min. The pellets were then washed using LiCl wash buffer (7-8times) and TE buffer (once). The pellet was then dissolved in IP elution buffer for 30 min at RT and then the supernatants were left at 65ºC overnight for reverse crosslinking. Next day the RNA and protein were digested with RNase and Proteinase K to obtain purified DNA. The DNA (150µg) isolated from $1X10^7$ cells was further processed for qPCR using specific primers for CIITApI, CIITApIII, CIITApIV and GAPDH promoter. The qPCR data were then normalized to input DNA. Primers for GAPDH promoter and antibody against mouse IgG both were used as negative controls [Table 2].

Cytokine Profiling

RAW 264.7 cells ($2X10^5$) were seeded onto 24 wells tissue culture plate and infected with *Msm* pSMT3 and *Msm esxL*. After 2 h of infection 20 mg/ml gentamycin containing DMEM media was added to kill the extracellular bacteria. After 1h the cells were then co-cultured with spleenocytes isolated from BALB/C mice. After 24 h the supernatant was harvested and cytokine levels were estimated using Bioplex kit assay (Bio-Rad).

Statistical analysis

All experiments were performed at least three times (n=3). Statistical analyses were performed using the Mann-Whitney U-test (two-tailed, equal variances). Significance was referred*** for P< 0.001 as ** for P $\leq$ 0.01 and * for P $\leq$ 0.05.

Acknowledgment

We would like to thank Sonawane lab members for fruitful discussions and critical reading of the manuscript. This work was supported by grant (AMR/44/2011-ECD-I) from Indian Council of Medical Research (ICMR), and grant (BT/PR5790/MED/29/602/2012) from Department of Biotechnology, Government of India to AS. Srabasti Sengupta is grateful to Department of Science and Technology, Government of India for awarding DST-INSPIRE fellowship (IF150081).

Conflict of Interest:

The authors declare that they have no conflicts of interest with the contents of this article.

Author's contributions

S. Sengupta planned the experimental setup, performed the experiments, analysed the data and wrote the manuscript. I Das, A Padhi, S Naik, G Ganguli, K Patnaik analyzed the experiments and provided technical assistance. S Naz constructed the esxL knockout (*Mtb* Δ*esxL)* mutant and performed the *Mtb* infection assay. V.K. Nandicoori supervised the construction of the knock out mutant and provided BSL3 lab facility. A Ahad contributed in performing the ChIP assay experiments and analysis of data. S K Raghav supervised the ChIP assay experiments and contributed in analyzing the data. A. Sonawane planned the experimental setup, data analysis, wrote the manuscript and provided all the necessary resources and support for the completion of the study. All authors reviewed the results and approved the final version of the manuscript.

References

1. Barros, S.P., and Offenbacher, S. (2014) Modifiable risk factors in periodontal disease: epigenetic regulation of gene expression in the inflammatory response. *Periodontol. 2000.* **64**, 95-110.
2. Esterhuyse, M.M., Linhart, H.G., and Kaufmann, S.H. (2012) Can the battle against tuberculosis gain from epigenetic research? *Trends. Microbiol*. **20**, 220-226.
3. Hamon, M.A., and Cossart, P. (2008) Histone modifications and chromatin remodeling during bacterial infections. *Cell. Host. Microbe*. **4**, 100-109.
4. Saccani, S., Pantano, S., and Natoli, G. (2002) p38-Dependent marking of inflammatory genes for increased NF-kappa B recruitment. *Nat. Immunol*. **3**, 69-75.
5. Basak, C., Pathak, S.K., Bhattacharyya, A., Pathak, S., Basu, J., and Kundu, M. (2005). The secreted peptidyl prolyl cis,trans-isomerase HP0175 of Helicobacter pylori induces apoptosis of gastric epithelial cells in a TLR4- and apoptosis signal-regulating kinase 1-dependent manner. *J. Immunol*. **174**, 5672–5680.
6. Schmeck, B., Beermann, W., van Laak, V., Zahlten, J., Opitz, B., Witzenrath, M., Hocke, A.C., Chakraborty, T., Kracht, M., Rosseau, S., Suttorp, N., and Hippenstiel, S. (2005) Intracellular bacteria differentially regulated endothelial cytokine release by MAPK-dependent histone modification. *J. Immunol*. 2005 Sep 1; 175(5):2843-50.
7. Hamon, M.A., Batsche, E., Regnault, B., Tham, T.N., Seveau, S., Muchardt, C., and Cossart, P. (2007). Histone modifications induced by a family of bacterial toxins. Proc. Natl. Acad. Sci. USA 104, 13467–13472.
8. Pathak, S.K., Basu, S., Bhattacharyya, A., Pathak, S., Banerjee, A., Basu, J., and Kundu, M. (2006). TLR4-dependent NF-kappaB activation and mitogenand stress-activated protein kinase 1-triggered phosphorylation events are central to Helicobacter pylori peptidyl prolyl cis-, trans-isomerase (HP0175)mediated induction of IL-6 release from macrophages. *J. Immunol.* **177**, 7950–7958.
9. WHO 2014 facts tuberculosis. http://www.who.int/mediacentre/factsheets/fs104/en/.
10. Boshoff, H. I., and Barry, C.E., 3rd. (2005) Tuberculosis: metabolism and respiration in the absence of growth. *Nat. Rev. Microbiol.* **3,** 70–80.

11. Pieters, J. (2001) Entry and survival of pathogenic mycobacteria in macrophages. *Microbes. Infect.* **3,** 249-255.
12. Cole, S.T., Brosch, R., Parkhill, J., Garnier, T., Churcher, C., Harris, D., Gordon, S.V., Eiglmeier, K., Gas, S., Barry, C.E. 3rd, Tekaia, F., Badcock, K., Basham, D., Brown, D., Chillingworth, T., Connor, R., Davies, R., Devlin, K., Feltwell, T., Gentles, S., Hamlin, N., Holroyd, S., Hornsby, T., Jagels, K., Krogh, A., McLean, J., Moule, S., Murphy, L., Oliver, K., Osborne, J., Quail, M.A., Rajandream, M.A., Rogers, J., Rutter, S., Seeger, K., Skelton, J., Squares, R., Squares, S., Sulston, J.E., Taylor, K., Whitehead, S., and Barrell, B.G. (1998) Deciphering the biology of Mycobacterium tuberculosis from the complete genome sequence. *Nature.* **393**, 537-544.
13. Rahman, M.A., Sobia, P., Dwivedi, V.P., Bhawsar, A., Singh, D.K., Sharma, P., Moodley, P., Van Kaer, L., Bishai, W.R., and Das, G. (2015) *Mycobacterium tuberculosis* TlyA Protein Negatively Regulates T Helper (Th) 1 and Th17 Differentiation and Promotes Tuberculosis Pathogenesis. *J. Biol. Chem.* **290**, 14407-14417.
14. Hickman, S.P., Chan, J., and Salgame, P. (2002) *Mycobacterium tuberculosis* induces differential cytokine production from dendritic cells and macrophages with divergent effects on naive T cell polarization. *J. Immunol*. **168**, 4636-4642.
15. Briken, V., and Miller, J.L. (2008) Living on the edge: inhibition of host cell apoptosis by *Mycobacterium tuberculosis*. *Future. Microbiol*. **3**, 415-422.
16. Kumar, P., Agarwal, R., Siddiqui, I., Vora, H., Das, G., and Sharma, P. (2012) ESAT6 differentially inhibits IFN-γ-inducible class II transactivator isoforms in both a TLR2-dependent and -independent manner. *Immunol. Cell. Biol.* **90**, 411-420.
17. Siddle, K.J., Deschamps, M., Tailleux, L., Nédélec, Y., Pothlichet, J., Lugo-Villarino, G., Libri, V., Gicquel, B., Neyrolles, O., Laval, G., Patin, E., Barreiro, L.B., and Quintana Murci, L. (2014) A genomic portrait of the genetic architecture and regulatory impact of microRNA expression in response to infection. *Genome. Res.* **24**, 850-859.
18. Esterhuyse, M.M., Linhart, H.G., and Kaufmann, S.H. (2012) Can the battle against tuberculosis gain from epigenetic research? *Trends. Microbiol*. **20**, 220-226.
19. Pennini, M.E., Pai, R.K., Schultz, D.C., Boom, W.H., and Harding, C.V. (2006) Mycobacterium tuberculosis 19-kDa lipoprotein inhibits IFN_induced chromatin remodeling of MHC2TA by TLR2 and MAPK signaling. *J. Immunol.* **176,** 4323–4330.
20. Boehm, U., Klamp, T., Groot, M., and Howard, J.C. (1997) Cellular responses to interferon-gamma. *Annu. Rev. Immunol*. **15**, 749-795.
21. Wang, Y., Curry, H.M., Zwilling, B.S., and Lafuse, W.P. (2005). Mycobacteria inhibition of IFN-gamma induced HLA-DR gene expression by up-regulating histone deacetylation at the promoter region in human THP-1 monocytic cells. *J. Immunol.* **174**, 5687–5694.
22. Rich, E. A., Torres, M., Sada, E., Finegan, C. K., Hamilton, B. D., and Toossi, Z. (1997) Mycobacterium tuberculosis (MTB)-stimulated production of nitric oxide by human alveolar macrophages and relationship of nitric oxide production to growth inhibition of MTB. *Tuber. Lung. Dis*. **78,** 247–255.
23. Shiloh, M.U., and Nathan, C.F. (2000) Reactive nitrogen intermediates and the pathogenesis of Salmonella and mycobacteria. *Curr. Opin. Microbiol.* **3**, 35-42.
24. Yang, C.S., Yuk, J.M., and Jo, E.K. (2009) The role of nitric oxide in mycobacterial infections. *Immune. Netw.* **9**, 46-52.
25. Ehrt, S., Schnappinger, D., Bekiranov, S., Drenkow, J., Shi, S., Gingeras, T. R., Gaasterland, T., Schoolnik, G., and Nathan, C. (2001) Reprogramming of the macrophage transcriptome in response to interferon-γ and Mycobacterium tuberculosis. Signaling roles of nitric-oxide synthase-2 and phagocyte oxidase. *J. Exp. Med.* **194,** 1123–1140.
26. Jagannath, C., Actor, J. K., and Hunter, R. L., Jr. (1998) Induction of nitric oxide in human monocytes and monocyte cell lines by Mycobacterium tuberculosis. *Nitric. Oxide.* **2,** 174–186.
27. MacMicking, J., Xie, Q. W., and Nathan, C. (1997) Nitric oxide and macrophage function. *Annu. Rev. Immunol.* **15,** 323–350.

28. Nicholson, S., Bonecini-Almeida Mda, G., Lapa e Silva, J. R., Nathan, C., Xie, Q. W., Mumford, R., Weidner, J. R., Calaycay, J., Geng, J., Boechat, N., Linhares, C., Rom, W., and Ho, J. L. (1996) Inducible nitric oxide synthase in pulmonary alveolar macrophages from patients with tuberculosis. *J. Exp. Med*. **183,** 2293–2302.
29. Serbina, N. V., Salazar-Mather, T. P., Biron, C. A., Kuziel, W. A., and Pamer, E. G. (2003) TNF/iNOS-producing dendritic cells mediate innate immune defense against bacterial infection. *Immunity*. **19,** 59–70.
30. Ghorpade, D.S., Holla, S., Sinha, A.Y., Alagesan, S.K., and Balaji, K.N. (2013) Nitric oxide and KLF4 protein epigenetically modify class II transactivator to repress major histocompatibility complex II expression during Mycobacterium bovis bacillus Calmette-Guerin infection. *J. Biol. Chem.* **288**, 20592-20606.
31. Brodin, P., Rosenkrands, I., Andersen, P., Cole, S.T., and Brosch, R. (2004) ESAT-6 proteins:protective antigens and virulence factors? *Trends. Microbiol*. **12,** 500-508.
32. Manzanillo, P.S., Shiloh, M.U., Portnoy, D.A., and Cox, J.S. *Mycobacterium tuberculosis* activates the DNA-dependent cytosolic surveillance pathway within macrophages. *Cell. Host. Microbe.* **11**, 469-480.
33. Simeone, R., Bobard, A., Lippmann, J., Bitter, W., Majlessi, L., Brosch, R., Enninga, J. (2012) Phagosomal rupture by *Mycobacterium tuberculosis* results in toxicity and host cell death. *PLoS. Pathog.* **8**, e1002507.
34. Geluk, A., van Meijgaarden, K.E., Franken, K.L., Subronto, Y.W., Wieles, B., Arend, S.M., Sampaio, E.P., de Boer, T., Faber, W.R., Naafs, B., and Ottenhoff, T.H. (2002) Identification and characterization of the ESAT-6 homologue of *Mycobacterium leprae* and T-cell cross-reactivity with *Mycobacterium tuberculosis*. *Infect. Immun*. **70**, 2544-2548.
35. Mohanty, S., Jagannathan, L., Ganguli, G., Padhi, A., Roy, D., Alaridah, N., Saha, P., Nongthomba, U., Godaly, G., Gopal, R.K., Banerjee, S., and Sonawane, A. (2015) A mycobacterial phosphoribosyltransferase promotes bacillary survival by inhibiting oxidative stress and autophagy pathways in macrophages and zebrafish. *J. Biol. Chem.* **290**, 13321-13343.
36. Padhi, A., Naik, S.K., Sengupta, S., Ganguli, G., and Sonawane, A. (2016) Expression of Mycobacterium tuberculosis NLPC/p60 family protein Rv0024 induce biofilm formation and resistance against cell wall acting anti-tuberculosis drugs in Mycobacterium smegmatis. *Microbes. Infect.* **18**, 224-236.
37. Mohanty, S., Dal Molin, M., Ganguli, G., Padhi, A., Jena, P., Selchow, P., Sengupta, S., Meuli, M., Sander, P., and Sonawane, A. (2016) Mycobacterium tuberculosis EsxO (Rv2346c) promotes bacillary survival by inducing oxidative stress mediated genomic instability in macrophages. *Tuberculosis (Edinb).* **96:**44-57.
38. Yaseen, I., Kaur, P., Nandicoori, V.K., and Khosla, S. (2015) Mycobacteria modulate host epigenetic machinery by Rv1988 methylation of a non-tail arginine of histone H3. *Nat. Commun.* 6, 8922.
39. Sethi, D., Mahajan, S., Singh, C., Lama, A., Hade, M.D., Gupta, P., and Dikshit, K.L. (2015) Lipoprotein, LprI, of Mycobacterium tuberculosis acts as a lysozyme inhibitor. *J. Biol. Chem*. pii: jbc.M115.662593.
40. Gu, S., Chen, J., Dobos, K.M., Bradbury, E.M., Belisle, J.T., and Chen, X. (2003) Comprehensive proteomic profiling of the membrane constituents of a *Mycobacterium tuberculosis* strain. *Mol. Cell. Proteomics.* **2**, 1284-1296.
41. Målen, H., Berven, F.S., Fladmark, K.E., and Wiker, H.G. (2007) Comprehensive analysis of exported proteins from *Mycobacterium tuberculosis* H37Rv. *Proteomics.* **7**, 1702-1718.
42. Pandey, H., Tripathi, S., Srivastava, K., Tripathi, D.K., Srivastava, M., Kant, S., Srivastava, K.K., and Arora, A. (2016) Characterization of culture filtrate proteins Rv1197 and Rv1198 of ESAT-6 family from Mycobacterium tuberculosis H37Rv. *Biochim Biophys Acta* **15**, pii: S0304-4165(16)30388-9.

43. Alderson, M.R., Bement, T., Day, C.H., Zhu, L., Molesh, D., Skeiky, Y.A., Coler, R., Lewinsohn, D.M., Reed, S.G., and Dillon, D.C. (2000) Expression cloning of an immunodominant family of *Mycobacterium tuberculosis* antigens using human CD4(+) T cells. *J. Exp. Med.* **191**, 551-560.
44. Jain, P., Hsu, T., Arai, M., Biermann, K., Thaler, D.S., Nguyen, A., González, P.A., Tufariello, J.M., Kriakov, J., Chen, B., Larsen, M.H., and Jacobs, W.R. Jr.(2014) Specialized transduction designed for precise high-throughput unmarked deletions in Mycobacterium tuberculosis. *MBio*. **5**, e01245-14.
45. Bose, M., Farnia, P., Sharma, S., Chattopadhya, D., and Saha, K. (1999) Nitric oxide dependent killing of mycobacterium tuberculosis by human mononuclear phagocytes from patients with active tuberculosis. *Int. J. Immunopathol. Pharmacol.* **12,**69-79.
46. Bogdan, C. (2001) Nitric oxide and the immune response. *Nat. Immunol.* **2,** 907–916.
47. Kanangat, S., Meduri, G.U., Tolley, E.A., Patterson, D.R., Meduri, C.U., Pak, C., Griffin, J.P., Bronze, M.S., and Schaberg, D.R. (1999) Effects of cytokines and endotoxin on the intracellular growth of bacteria. *Infect. Immun.* **67**, 2834-2840.
48. Singh, G., Singh, B., Trajkovic, V., and Sharma, P. (2005) Mycobacterium tuberculosis 6 kDa early secreted antigenic target stimulates activation of J774 macrophages. *Immunol. Lett.* **98**, 180-188.
49. Pai, R.K., Convery, M., Hamilton, T.A., Boom, W.H., and Harding, C.V. (2003) Inhibition of IFN-gamma-induced class II transactivator expression by a 19-kDa lipoprotein from Mycobacterium tuberculosis: a potential mechanism for immune evasion. *J. Immunol*. **171**, 175-184.
50. Chang, C.H., Guerder, S., Hong, S.C., van Ewijk, W., and Flavell, R.A. (1996) Mice lacking the MHC class II transactivator (CIITA) show tissue-specific impairment of MHC class II expression. *Immunity*. **4**, 167-178.
51. Nelson, B.H. (2004) IL-2, regulatory T cells, and tolerance. *J. Immunol*. **172**,3983-3988.
52. Boyman, O., and Sprent, J. (2012) The role of interleukin-2 during homeostasis and activation of the immune system. *Nat. Rev. Immunol.* **12**, 180-190.
53. Pennini, M.E., Liu, Y., Yang, J., Croniger, C.M., Boom, W.H., and Harding, C.V. (2007). CCAAT/enhancer-binding protein beta and delta binding to CIITA promoters is associated with the inhibition of CIITA expression in response to Mycobacterium tuberculosis 19-kDa lipoprotein. *J. Immunol*. **179**, 6910–6918.
54. Bannister, A.J., Zegerman, P., Partridge, J.F., Miska, E.A., Thomas, J.O., Allshire, R.C., and Kouzarides, T. (2001) Selective recognition of methylated lysine 9 on histone H3 by the HP1 chromo domain. *Nature*. **410**, 120-124.
55. Fritsch, L., Robin, P., Mathieu, J.R., Souidi, M., Hinaux, H., Rougeulle, C., Harel-Bellan, A., Ameyar-Zazoua, M., and Ait-Si-Ali, S. (2010) A subset of the histone H3 lysine 9 methyltransferases Suv39h1, G9a, GLP, and SETDB1 participate in a multimeric complex. *Mol Cell.* **37**, 46-56.
56. Tachibana, M., Sugimoto, K., Nozaki, M., Ueda, J., Ohta, T., Ohki, M., Fukuda, M., Takeda, N., Niida, H., Kato, H., and Shinkai, Y. (2002) G9a histone methyltransferase plays a dominant role in euchromatic histone H3 lysine 9 methylation and is essential for early embryogenesis. *Genes. Dev.* **16**, 1779-1791.
57. Kapoor, N., Narayana, Y., Patil, S. A., and Balaji, K. N. (2010) Nitric oxide is involved in Mycobacterium bovis bacillus Calmette-Guerin-activated Jagged1 and Notch1 signaling. J. Immunol. **184,** 3117–3126.
58. Bansal, K., and Balaji, K. N. (2011) Intracellular pathogen sensor NOD2 programs macrophages to trigger Notch1 activation. J. Biol. Chem. **286,** 5823–5835.
59. Vermeulen, L., Vanden Berghe, W., Beck, I.M., De Bosscher, K., and Haegeman, G. (2009) The versatile role of MSKs in transcriptional regulation. *Trends. Bioche. Sci.* **34**, 311-318.
60. Yang, S.H., Vickers, E., Brehm, A., Kouzarides, T., and Sharrocks, A.D. (2001). Temporal recruitment of the mSin3A-histone deacetylase corepressor complex to the ETS domain transcription factor Elk-1. *Mol. Cell. Biol.* **21**, 2802–2814.

61. Schorey, J.S., and Cooper, A.M. (2003) Macrophage signalling upon mycobacterial infection: the MAP kinases lead the way. *Cell. Microbiol*. **5**, 133-142.
62. de Jonge, M.I., Pehau-Arnaudet, G., Fretz, M.M., Romain, F., Bottai, D., Brodin, P., Honoré, N., Marchal, G., Jiskoot, W., England, P., Cole, S.T., and Brosch, R. (2007) ESAT-6 from Mycobacterium tuberculosis dissociates from its putative chaperone CFP-10 under acidic conditions and exhibits membrane-lysing activity. *J. Bacteriol.* **189**, 6028-6034.
63. Renshaw, P.S., Lightbody, K.L., Veverka, V., Muskett, F.W., Kelly, G., Frenkiel, T.A., Gordon, S.V., Hewinson, R.G., Burke, B., Norman, J., Williamson, R.A., and Carr, M.D. (2005) Structure and function of the complex formed by the tuberculosis virulence factors CFP-10 and ESAT-6. *EMBO J*. **24**, 2491-2498.
64. Derrick, S.C., and Morris, S.L. (2007) The ESAT6 protein of Mycobacterium tuberculosis induces apoptosis of macrophages by activating caspase expression. *Cell. Microbiol*. **9,** 1547-1555.
65. Choi, H.H., Shin, D.M., Kang, G., Kim, K.H., Park, J.B., Hur, G.M., Lee, H.M., Lim, Y.J., Park, J.K., Jo, E.K., and Song, C.H. (2010) Endoplasmic reticulum stress response is involved in Mycobacterium tuberculosis protein ESAT-6-mediated apoptosis. *FEBS Lett.* **584**, 2445-2454.
66. Brodin, P., Rosenkrands, I., Andersen, P., Cole, S.T., and Brosch, R. (2004) ESAT-6 proteins: protective antigens and virulence factors? *Trends. Microbiol*. **12**, 500-508.
67. De Leon, J., Jiang, G., Ma, Y., Rubin, E., Fortune, S., and Sun, J. (2012) *Mycobacterium tuberculosis* ESAT-6 exhibits a unique membrane-interacting activity that is not found in its ortholog from non-pathogenic *Mycobacterium smegmatis*. *J. Biol. Chem.* **287**, 44184-44191.
68. Marongiu, L., Donini, M., Toffali, L., Zenaro, E., and Dusi, S. (2013) ESAT-6 and HspX improve the effectiveness of BCG to induce human dendritic cells-dependent Th1 and NK cells activation. *PLoS One.* **8,** e75684.
69. Fishbein, S., van Wyk, N., Warren, R.M., and Sampson, S.L. (2015) Phylogeny to function: PE/PPE protein evolution and impact on Mycobacterium tuberculosis pathogenicity. *Mol. Microbiol*. **96**, 901-916.
70. Chumduri, C., Gurumurthy, R.K., Zadora, P.K., Mi, Y., and Meyer, T.F. (2013) Chlamydia infection promotes host DNA damage and proliferation but impairs the DNA damage response. *Cell. Host. Microbe*. 13, 746-758.
71. Saini, N.K., Sharma, M., Chandolia, A., Pasricha, R., Brahmachari, V., and Bose, M. (2008) Characterization of Mce4A protein of *Mycobacterium tuberculosis*: role in invasion and surviv al. *BMC Microbiol*. **8**, 200.
72. Tiwari, B.M., Kannan, N., Vemu, L., and Raghunand, T.R. (2012) The *Mycobacterium tuberculosis* PE proteins Rv0285 and Rv1386 modulate innate immunity and mediate bacillary survival in macrophages. *PLoS One.* **7**, e51686.
73. Kumar, A., Farhana, A., Guidry, L., Saini, V., Hondalus, M., and Steyn, A.J. (2011) Redox homeostasis in mycobacteria: the key to tuberculosis control? *Expert. Rev. Mol. Med*. **13**, e39.
74. Voskuil, M.I., Bartek, I.L., Visconti, K., and Schoolnik, G.K. (2011) The response of *Mycobacterium tuberculosis* to reactive oxygen and nitrogen species. *Front. Microbiol*. **2**, 105.
75. Lamichhane, G. (2011) *Mycobacterium tuberculosis* response to stress from reactive oxygen and nitrogen species. *Front. Microbiol.* **27**, 176.
76. Firmani, M.A., and Riley, L.W. (2002) Reactive nitrogen intermediates have a bacteriostatic effect on Mycobacterium tuberculosis in vitro. *J. Clin. Microbiol*. **40,** 3162-3166.
77. Harding, C.V., and Boom, W.H. (2010) Regulation of antigen presentation by Mycobacterium tuberculosis: a role for Toll-like receptors. *Nat. Rev. Microbiol*. **8**, 296-307.
78. Pattenden, S. G., Klose, R., Karaskov, E., and Bremner, R. (2002) Interferon_-induced chromatin remodeling at the CIITA locus is BRG1 dependent. EMBO J. **21,** 1978–1986
79. Zika, E., Greer, S. F., Zhu, X. S., and Ting, J. P. (2003) Histone deacetylase 1/mSin3A disrupts interferon-induced CIITA function and major histocompatibility complex class II enhanceosome formation. Mol. Cell. Biol. **23,** 3091–3102.

80. Jung, S.B., Yang, C.S., Lee, J.S., Shin, A.R., Jung, S.S., Son, J.W., Harding, C.V., Kim, H.J., Park, J.K., Paik, T.H., Song, C.H., and Jo, E.K. (2006) The mycobacterial 38-kilodalton glycolipoprotein antigen activates the mitogen-activated protein kinase pathway and release of proinflammatory cytokines through Toll-like receptors 2 and 4 in human monocytes. *Infect. Immun.* **74**, 2686-2696.
81. Jena, P., Mohanty, S., Mohanty, T., Kallert, S., Morgelin, M., Lindstrøm, T., Borregaard, N., Stenger, S., Sonawane, A., and Sørensen, O.E. (2012) Azurophil granule proteins constitute the major mycobactericidal proteins in human neutrophils and enhance the killing of mycobacteria in macrophages. *PLoS One*. **7**, e50345.
82. Soni, V., Upadhayay, S., Suryadevara, P., Samla, G., Singh, A., Yogeeswari, P., Sriram, D., and Nandicoori, V.K. (2015) Depletion of *M. tuberculosis* GlmU from Infected Murine Lungs Effects the Clearance of the Pathogen. *PLoS Pathog*.**11**, e1005235.

Figure legends

Figure 1: Genetic organization, growth analysis, bacterial survival and *Mtb* Δ*esxL* mutant construction. (**A)** Schematic representation of e*sxL* in the *M. tuberculosis* H37Rv genome. RAW264.7 **(B)** and THP-1 **(C)** were infected with *Msm* pSMT3 and recombinant *Msm esxL* strains. The cells were lysed, and intracellular survival was determined 1, 8, and 24 h post-infection by a cfu assay. (**D)** *In-vitro* growth curve of the *Msm* WT, *Msm* pSMT3 and recombinant *Msm esxL* was determined by growing bacteria in 7H9 medium and measuring O.D. ($A_{600\ nm}$). **(E)** Extracellular expression of *esxL* transcript was measured by qRT-PCR after growing *Msm esxL in-vitro* for 4, 12 and 24 h. RNA was isolated at different time points. cDNA was synthesized and the expression of *esxL* was determined using qRT-PCR. Transcript levels are represented relative to mRNA levels of *Msm esxL* at 4 h which is assigned a value of 1. The expression values were normalized with *sigA*. **(F)** Intracellular expression of *esxL* transcript was measured by qRT-PCR. RNA was isolated from *Msm esxL* infected macrophages at different time points. cDNA was synthesized and the expression of *esxL* was determined using qRT PCR. Transcript levels are represented relative to mRNA levels of *Msm esxL* at 4 h which is assigned a value of 1. The expression values were normalized with *sigA*. (**G)** Schematic representation of construction of *Mtb* Δ*esxL* mutant by homologous recombination. The location of primers used for the confirmation of deletion mutant generation is depicted. **(H)** Confirmation of *Mtb* Δ*esxL* mutant generation. F1 and R2 primers were designed beyond the flanks, whereas R1 and F2 primers anneal to *sacB-hyg*^{r} cassette. PCR using F1 and R1 is expected to give no product with the *Mtb* (lane 1) and ~1.3 kb with the *Mtb* Δ*esxL* (lane 2); F2-R2 primer sets were expected to give no product with *Mtb* and ~1.5 kb in *Mtb* Δ*esxL* mutant. Amplificaiton of *udgB* with gene specific primers was performed as a control. The experiments were performed in triplicate (n=3). Results are shown as mean ± S.D. ***, $p \leq 0.001$; **, $p \leq 0.01$; *, $p \leq 0.05$.; ns, not significant.

Figure 2: Determination of NO production and iNOS expression *in Msm pSMT3, Msm esxL, Mtb* H37Rv *and Mtb* Δ*esxL* infected cells. (A) RAW264.7 cells were infected with *Msm pSMT3* and recombinant *Msm esxL* for 48 h. The production of NO was quantified using Griess reagent. **(B)** The level of iNOS expression at mRNA level was quantified by using Real time PCR. Transcript levels of *iNOS* in *Msm* pSMT3 and *Msm esxL* infected macrophages were determined by qRT-PCR 24 h post infection. *GAPDH* was taken as internal control. **(C)** and **(D)** iNOS expression was checked by Western blotting **(C)** and fluorescence microscopic (D) analysis using iNOS specific antibody in *Msm pSMT3* and *Msm esxL* infected macrophages. **(E)** THP-1 cells were infected with *Mtb* and *Mtb* Δ*esxL* mutant for 24 h. The level of iNOS was checked by Western blotting. The experiments were performed in triplicate (n=3). Results are shown as mean ± S.D. ***, $p \leq 0.001$; **, $p \leq 0.01$; *, $p \leq 0.05$.

Figure 3: Expression of CIITA and MHC-II in *Msm pSMT3, Msm esxL, Mtb* H37Rv and ***Mtb* Δ*esxL* infected macrophages. (A)** RAW264.7 cells were infected with *Msm* pSMT3 and recombinant *Msm esxL* for 24 h. The transcript level of *CIITA* was quantified by using qRT-PCR. Uninfected cells were used as control**. (B)** RAW264.7 cells were infected with *Msm* pSMT3 and recombinant *Msm esxL* for 48 h. Cell lysates were prepared at indicated time points. CIITA expression was checked by Western blotting. **(C)** The level of CIITA after *Mtb* infection was checked by Western blotting. Expression of CIITA protein was determined in *Mtb* H37Rv infected THP-1 cells by Western blotting using an antibody specific to CIITA after 24, 48 and 72 h of infection. The Western blot and densitometry analysis shown is representative of at least two biological replicates. **(D)** Western blot analysis to check expression CIITA in THP-1 cells infected with *Mtb* and *Mtb* Δ*esxL* after 48 h of infection. The expression level of MHC-II was checked at both transcriptional **(E)** and translational **(F)** levels in RAW 264.7 cells infected with *Msm* pSMT3 and recombinant *Msm esxL* strains for 24 h. **(G)** THP-1 and **(H)** RAW 264.7 cells were infected with *Msm* pSMT3 and recombinant *Msm esxL* strains for 24 h. Flowcytometric analysis of MHC-II expression was determined by using anti-MHCII antibody and analyzed through 10,000 gated cells. **(I)** Expression of MHCII protein was determined in *Mtb* H37Rv infected THP-1 cells by Western blotting using an antibody

specific to MHCII after 24, 48 and 72 h of infection. **(J)** The level of MHCII was checked in *Mtb* H37Rv and *Mtb* Δ*esxL* infected THP-1 cells by Western blotting after 24 and 48 h of infection. For qRT-PCR, *GAPDH* was taken as an internal control. The experiments were performed in triplicate (n=3). Results are shown as mean ± S.D. (error bars); **, $p \leq 0.01$.

Figure 4: Analysis of IL-2, IL-6, IL-10 and TNF-α cytokines in RAW 264.7 and spleenocyte co-cultured cells infected with *Msm* pSMT3 and recombinant *Msm esxL* strains. The level of IL-2 (A), IL-10 (B), TNF-α (C) and IL-6 (D) cytokines was determined by using Bioplex cytokine analysis kit. Infected RAW 264.7 cells were co-cultured with spleenocytes isolated from BALB/C mice in presence and absence G9a inhibitor (UNC0638) and cell supernants were collected after 24 of infection. The experiments were performed in triplicate (n=3). Results are shown as mean ± S.D. (error bars); **, $p \leq 0.01$; *, $p \leq 0.05$.

Figure 5: Expression of H3K9me2/3 in macrophages. RAW264.7 cells were infected with *Msm* pSMT3 and recombinant *Msm esxL* for 24 h. The expression of H3K9me2/3 was determined by Western blotting **(A)** and fluorescence microscopy **(B)**. **(C)** Western blot analysis of H3K4me3 and total H3 was performed in *Msm* pSMT3 and recombinant *Msm esxL* infected macrophages after 24 h of infection. **(D)** Expression of H3K9me2/3 was determined in *M. bovis*-BCG infected RAW 264.7 cells in presence and absence of G9a inhibitor (UNC0638) after 24 h infection. **(E)** The level of H3K9me2/3 was determined in *Mtb* H37Rv infected THP-1 by Western blotting using an antibody specific to H3K9me2/3 after 24, 48 and 72 h of infection. **(F)** Differentiated THP-1 cells were infected with *Mtb* and *Mtb* Δ*esxL* for 48 h. The level of H3K9me2/3 was checked by Western blotting. The level of G9a expression was checked in *Msm* pSMT3 and recombinant *Msm esxL* infected RAW 264.7 cells **(G)** and *Mtb* and *Mtb* Δ*esxL* infected THP-1 cells **(H)** by qRT-PCR. **(I)** RAW264.7 cells were treated with UNC0638 (G9a inhibitor) followed by infection with *Msm* pSMT3 and recombinant *Msm esxL*. Expressions of CIITA and H3K9me2/3 were checked by Western blotting after 24 h of infection. ChIP assay was performed to check the H3K9me2/3 enrichment at CIITA promoter (pIV) after infecting RAW264.7 cells with *Msm* pSMT3 and recombinant *Msm esxL* **(J)** and after treatment with G9a inhibitor **(K)** for 24 h. Quantification of the data was done by qRT-PCR using specific ChIP primers. *GAPDH* was taken as an internal control for qRT-PCR. GAPDH promoter was taken as an additional negative control for ChIP qRT-PCR. The experiments were performed in triplicate (n=3). Results are shown as mean ± S.D. (error bars); ***, $p \leq 0.001$; **, $p \leq 0.01$; *, $p \leq 0.05$; ns, not significant.

Figure 6: Role of P38, ERK and iNOS in CIITA and H3K9me3 expression. RAW264.7 cells were infected with *Msm* pSMT3 and recombinant *Msm esxL* for 24 h. The expression of p-P38 **(A)** and p-ERK **(B)** was estimated by Western blotting. (C) THP-1 cells were infected with *Mtb* and *Mtb* Δ*esxL* for 24 h and the level of p-P38 was determined by Western blotting. The level of H3K9me2/3 and CIITA was checked by Western blotting. The expression of CIITA and H3K9me3 was checked in *Msm* pSMT3 and recombinant *Msm esxL* infected cells after treatment with SB203580 (P38 inhibitor) **(D)** and U0126 (ERK inhibitor) **(E)**. **(F)** The expression of CIITA, H3K9me3 and iNOS was checked in *Msm* pSMT3 and recombinant *Msm esxL* infected cells after treatment with 1400W (iNOS inhibitor). The experiments were performed in triplicate (n=3).

Figure 7: Schematic representation of role of *Mtb esxL* in induction of hyper-methylation of H3K9, which down regulates the expression of CIITA, the major co-activator of MHCII. This results in down-regulation of MHCII expression, and reduced production of IL2.

Table 1: Oligos used in this study

Sl no.	Primer Name	Sequence (5'>>3')
1.	esxL FP	GTCCCTGCAGGATGACCATCAACTATC
2.	esxL RP	GTCCAAGCTTTCAGGCCCAGCTGGAG
3.	iNOS FP	TTC CAA GAG CCT TGC TGT TT
4.	iNOS RP	GTA GGT AAG GGC GTT GGT CA
5.	CIITA FP	ACGCTTTCTGGCTGGATTAGT
6 .	CIITA RP	TCAACGCCAGTCTGACGAAGG
7.	MHCII FP	TGGGCACCATCTTCATCATTC
8.	MHCII RP	GGTCACCCAGCACACCACTT
9.	GAPDH FP	GAGAGGCCCTATCCCAACTC
10.	GAPDH RP	TTCACCTCCCCATACACACC
11.	esxL FP	GTTGACCGCGAGTGACTTTT
12.	esxL RP	GGTTTGCGCCATGTTGTT
13.	SigA FP	CCAAGGGCTACAAGTTCTCG
14.	SigA RP	TGGATCTCCAGCACCTTCTC

Table 2: Oligos used in ChIP assay

Sl no.	Primer Name	Sequence (5'>>3')
1.	CIITApI FP	GCATAGCAGATGCAAAACCA
2.	CIITApI RP	GGGCAGATTATTACAGATTAGTTGC
3.	CIITApIII FP	ACGTCCAGAGAAACTCAATGC
4.	CIITApIII RP	AGAGCTGTTAGGGACATGGTG
5.	CIITApIV FP	CTACTGGCTCAAATCTGTCGTC
6.	CIITApIV RP	CAGGCAGATCTCACTTAGACCA
7.	GAPDHpromoter FP	GGATAGAATGTAGCCCTGGACTT
8.	GAPDHpromoter RP	TGTGCATGTATCTTTATTGGCTCT

Figure 1

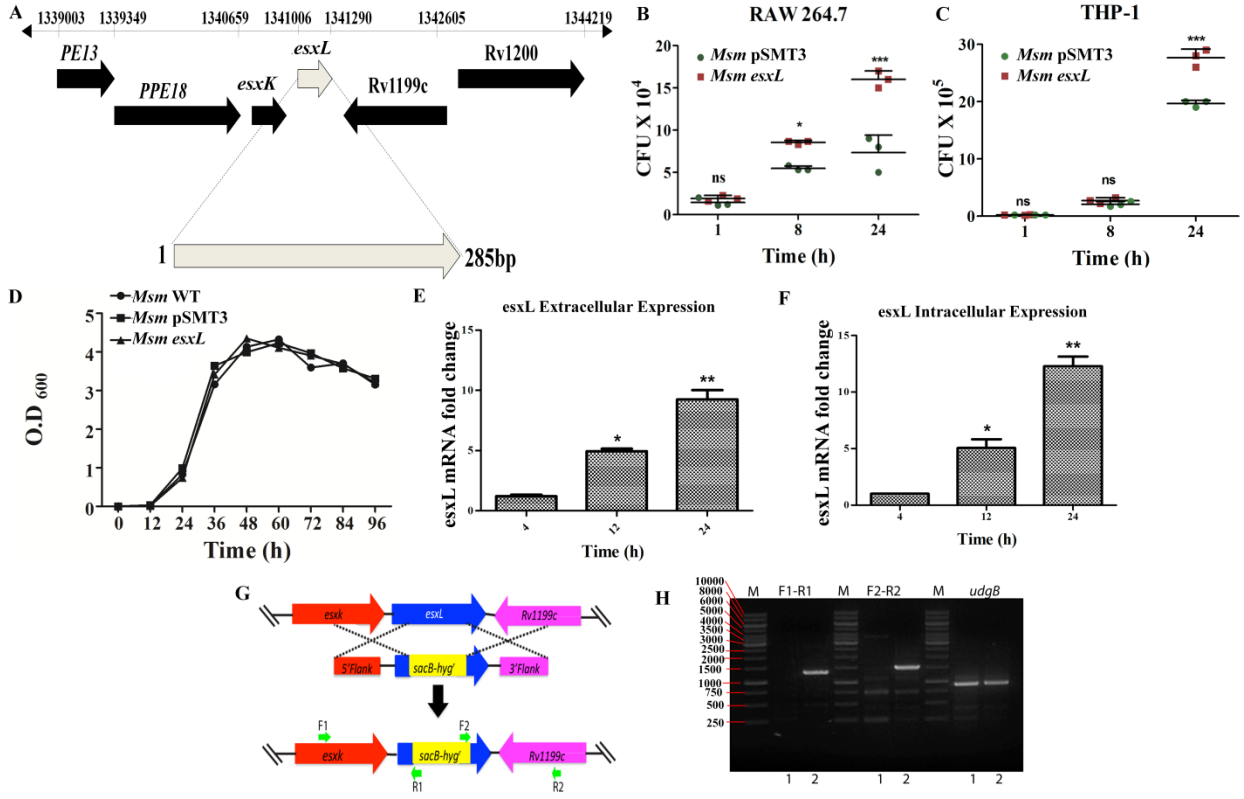

Figure 2

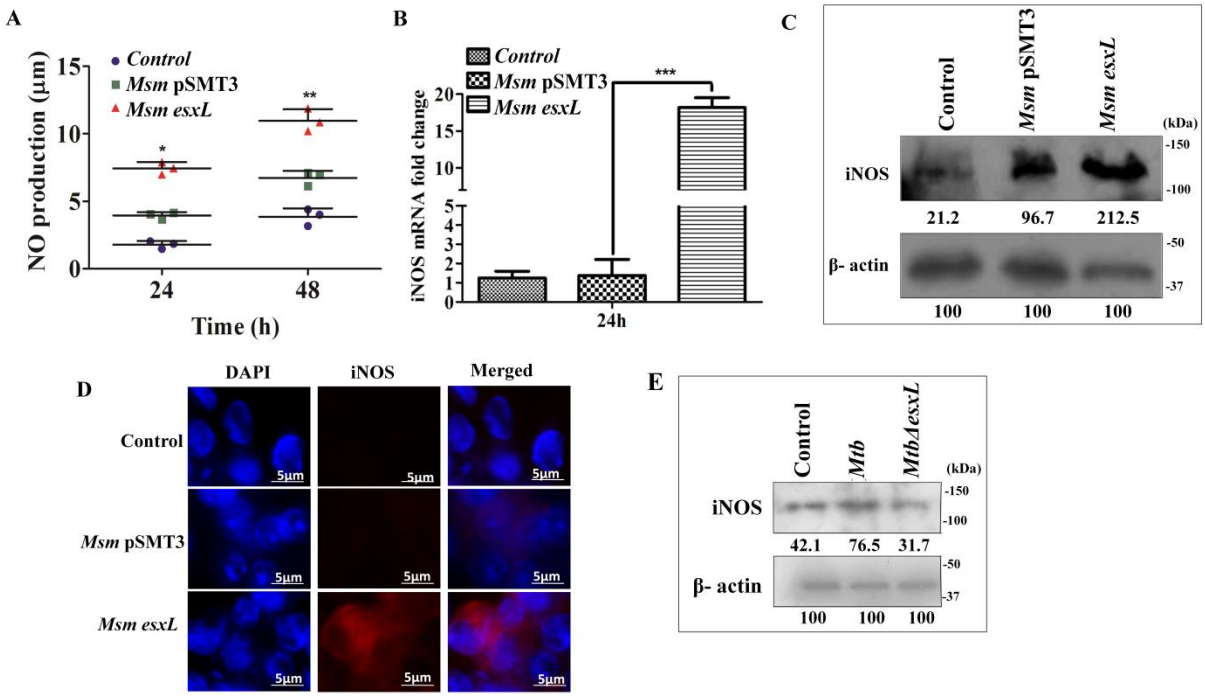

Figure 3

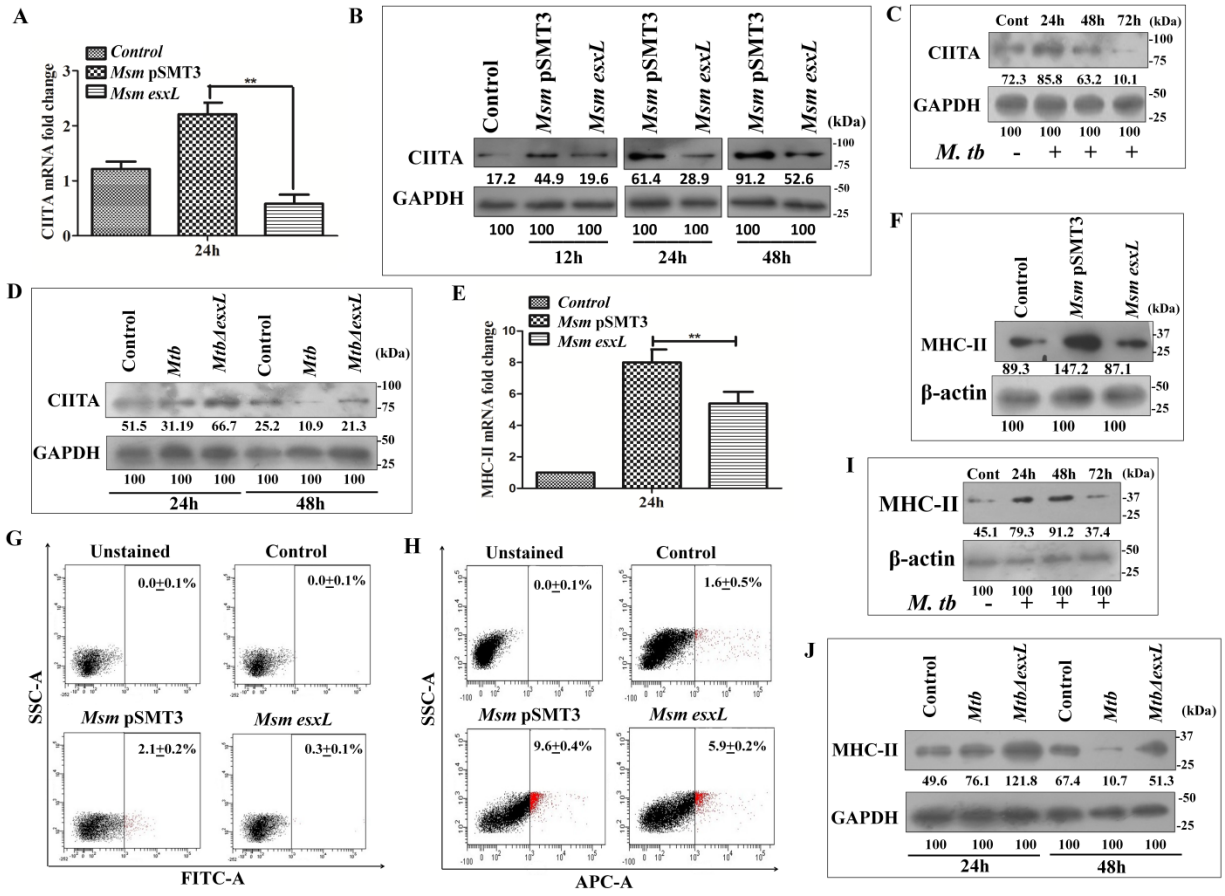

Figure 4

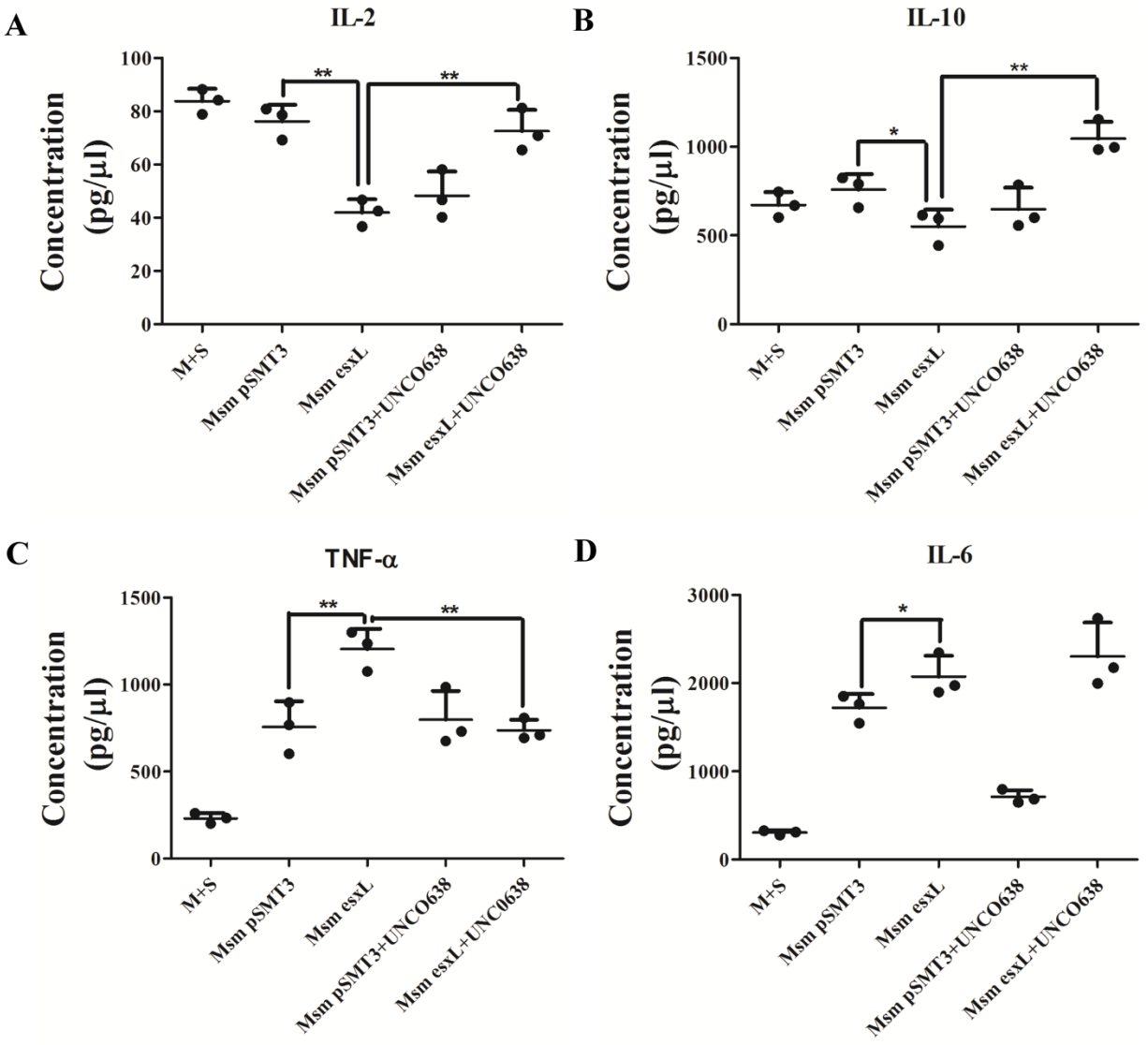

Figure 5

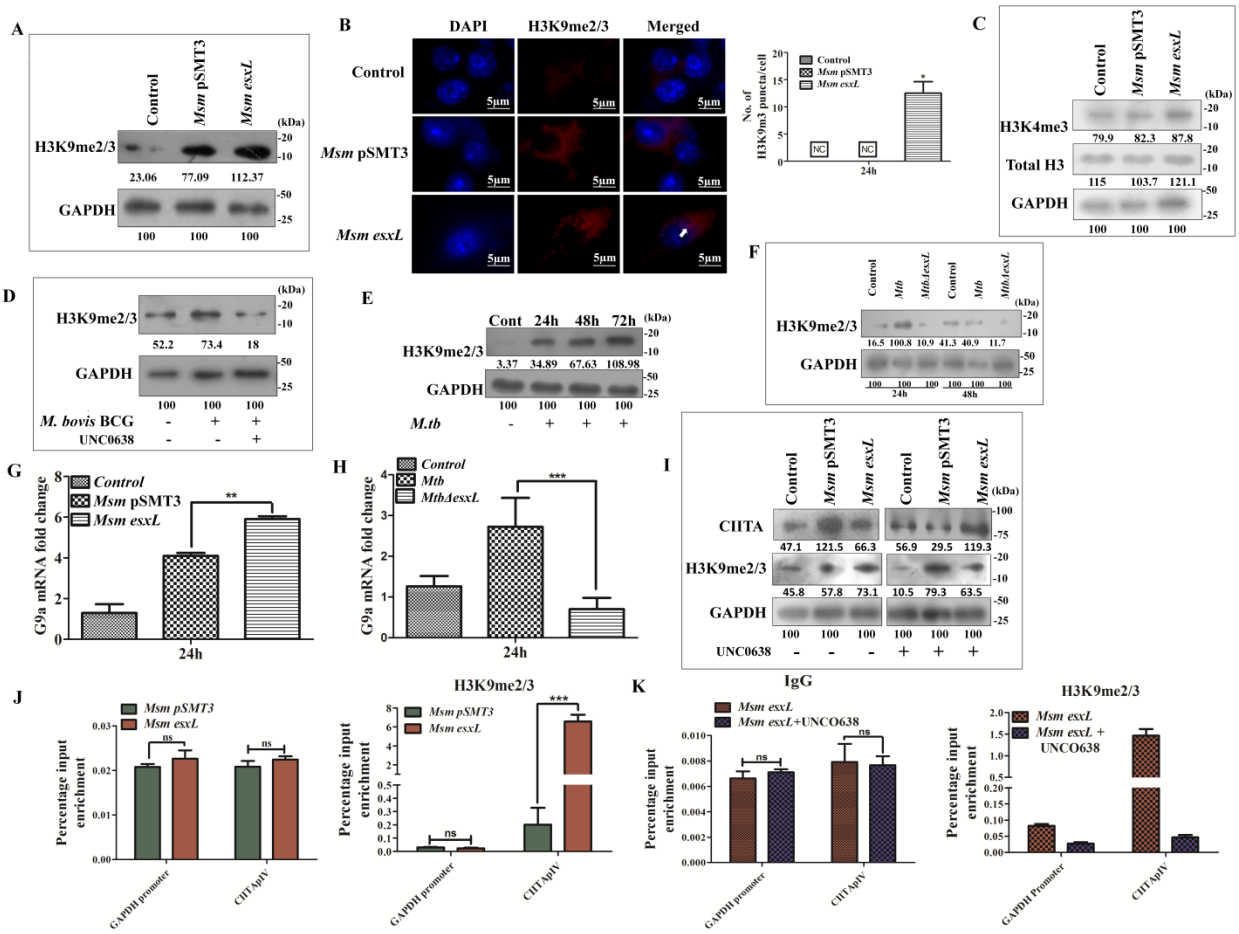

Figure 6

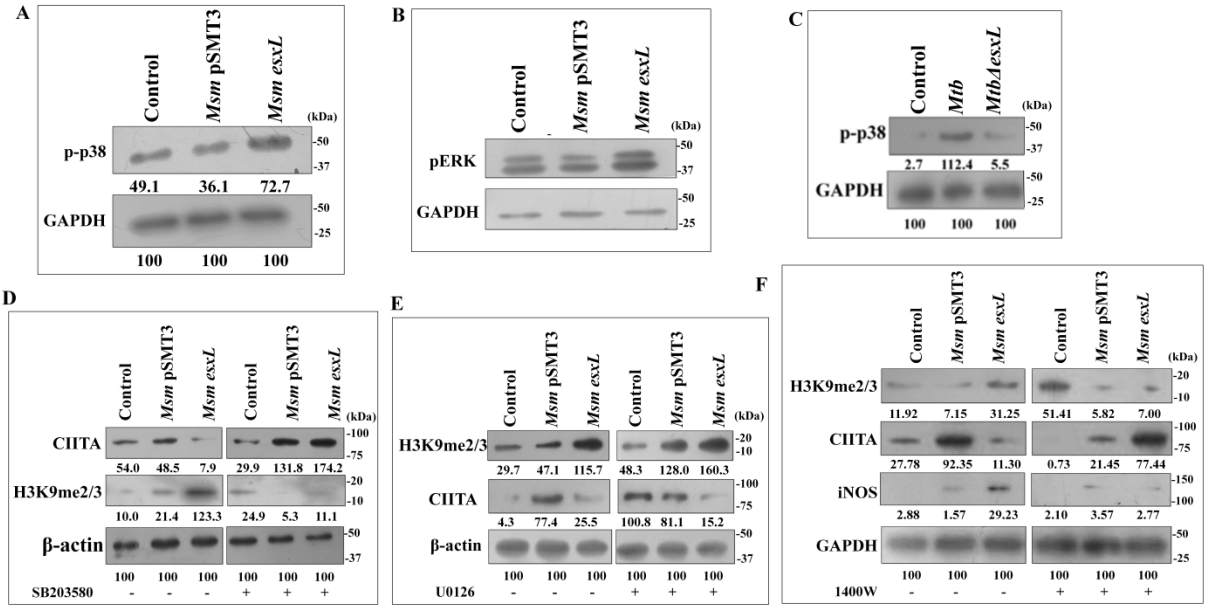

Figure 7

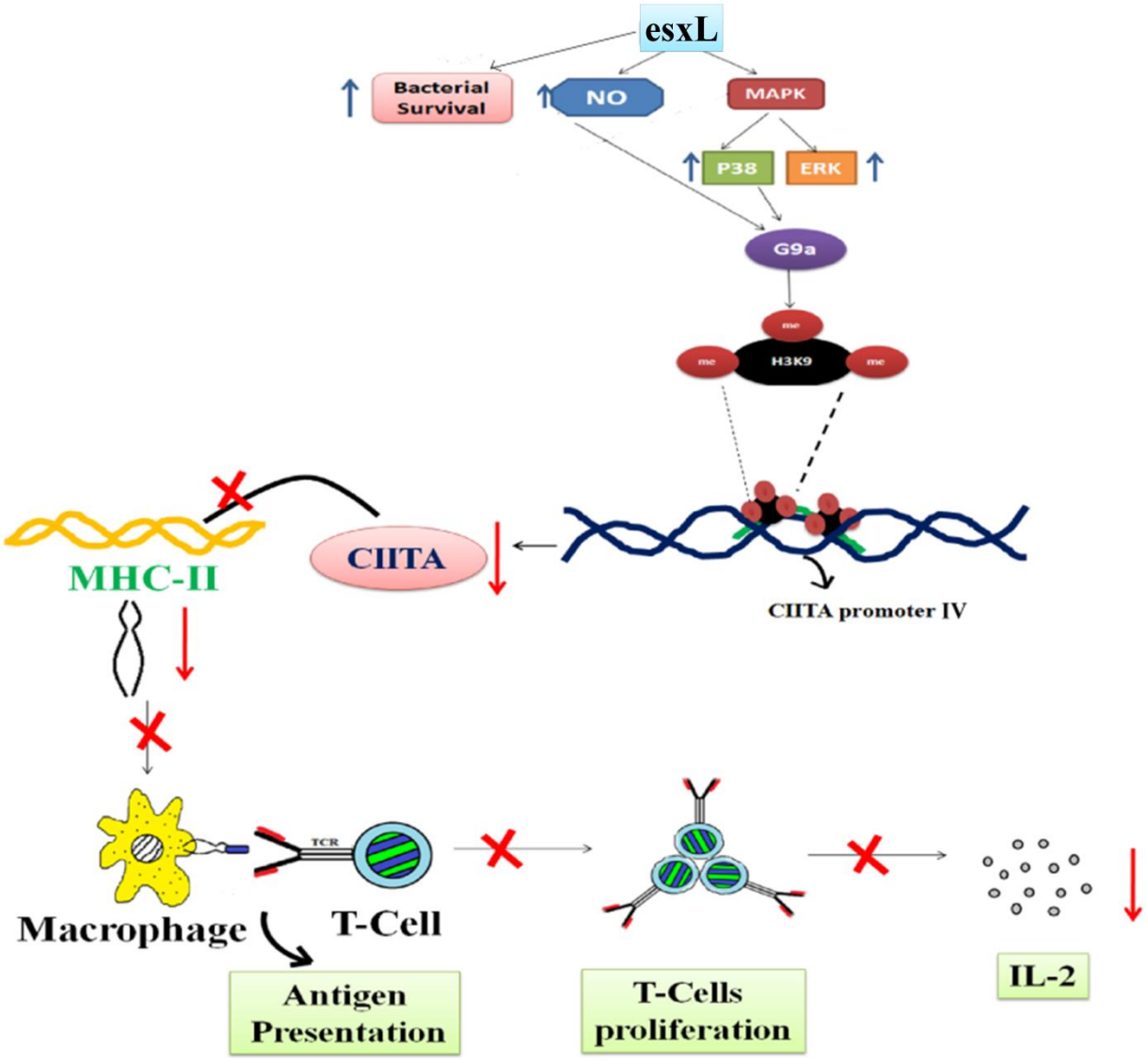

Mycobacterium tuberculosis esxL inhibit MHC-II expression by promoting hypermethylation in class-II transactivator loci in macrophages

Srabasti Sengupta, Saba Naz, Ishani Das, Abdul Ahad, Avinash Padhi, Sumanta Naik, Geetanjali Ganguli, Kaliprasad Patnaik, Sunil Kumar Raghav, Vinay Nandicoori and Avinash Sonawane

J. Biol. Chem. published online February 16, 2017

Access the most updated version of this article at doi: 10.1074/jbc.M117.775205